Exp. Theo. NANOTECHNOLOGY 10 (2026) 585-592 https://doi.org/10.56053/10.2.585

Using laser ablation at different laser energies for synthesis and characterization of TiO_2 thin films nanoparticles

Rusul M. Abdallah, Aws K. Mohammed, Holya A. Lafta, Nura A. Abdulzahara*

Department of Medical Physics, College of Sciences, Al-karkh University of Science, Baghdad, Iraq
*) Email: rusul.mohammed@kus.edu.iq

Received 10/2/2026, *Received in revised form* 17/3/2026, *Accepted* 26/3/2026, *Published* 15/4/2026

Titania (TiO_2) is one of the most studied nano-materials due to its unique properties and applications across diverse areas, including photocatalysis, hydrogen production, energy conservation, self-cleaning coatings, and solar cells. This study uses a novel, environmentally friendly approach to generate TiO_2 thin-film nanoparticles in 5 min via one-step laser ablation of titanium powder into nanometer-scale structures in deionized water. This top-down approach allows it to improve nanoparticle properties by adjusting laser parameters, especially laser energy, which is very important for determining the size distribution, crystalline structure, and optical band-gap behavior of the particles. The X-ray diffraction patterns of TiO_2 thin film nanoparticles indicate the formation of the rutile phase. Increasing laser energy sharpens the diffraction peaks and reduces the full width at half maximum, indicating improved crystallinity and increased crystallite size. The FESEM image confirms that all the samples have spherical to quasi-spherical nanoparticles with noticeable agglomeration. The nanoparticles exhibit consistent morphology, and the majority of nanoparticles fall within the 20–70 nm range. The UV-Vis absorption spectra of the samples are measured at different laser energies. It exhibits absorption bands at 295, 298, 297, and 296 nm for 50, 100, 150, and 250 mJ, respectively. From these bands of absorption, the absorption increased with increasing laser energy. Results indicate that as the laser energy increases, the nanoparticles' size increases significantly. The particle size and shape are influenced by laser energy.

Keywords: TiO_2 NPs; Laser ablation; Physical properties.

1. INTRODUCTION

Titania (TiO_2) is a significant nano-material that has attracted substantial interest owing to its distinctive properties [1]. Titanium dioxide nanoparticles (TiO_2 NPs) have garnered significant interest

due to their diverse uses in photocatalysis, hydrogen production, energy conservation, self-cleaning coatings, and solar cells [2]. TiO_2 occurs in three primary crystalline polymorphs: anatase (tetragonal, metastable), rutile (tetragonal, thermodynamically stable), and brookite (orthorhombic, metastable)[1–3].TiO_2 NPs are excellent semiconductor materials for solar cells because they are chemically very stable, non-toxic, economical, and highly effective photocatalysts for breaking down organic pollutants [4]. Additionally, TiO_2 nanoparticles are commonly employed as photoanode materials owing to their excellent light absorption, particularly in the ultraviolet range, advantageous chemical solubility, exceptional photo-corrosion resistance, and cost-effectiveness [5]. TiO_2 is widely used as a photocatalyst because its energy band gap is less than 3.5 eV [6–8].

There are many ways to synthesize Titania and Titania-based nano-materials, including the sol-gel method [9], solvothermal method [9], hydrothermal method [10], chemical vapor deposition (CVD) [11], direct oxidation [12], electrodeposition [13], sonochemistry [14], and microwaves [14]. These methods are primarily used to produce TiO_2 nanostructured materials. One of the most widely used methods for producing TiO_2 NPs is laser ablation in liquids, which makes it easier to grow and modify [15]. Laser ablation is a novel method for producing TiO_2 nanoparticles that is safe and environmentally friendly[16]. It converts bulk titanium metal into oxide nanoparticles via high-energy interactions between laser light and water [17]. Laser ablation in liquid media refers to the use of different kinds of lasers to ablate a solid target in a liquid solvent. The production of TiO_2 nanoparticles is significantly influenced by important laser parameters, such as energy, pulse length, and wavelength. Higher energy levels promote the rutile phase and speed up crystallization, particularly when deionized water is used. Avoiding clumping is crucial when utilizing these nanoparticles in solutions. [15–17].

Many studies provide insight into methods for generating TiO_2 nanoparticles. For example, A. Singh et al. [18] used pulsed laser ablation to produce TiO_2 nanoparticles in water and wrote about how the intensity of the laser affected the TiO_2 nanoparticles that are produced. The produced TiO_2 nanoparticles showed an increase in yield with increasing laser power. Huang et al. [19] investigated TiO_2 nanoparticles synthesized via the PLAL approach on a titanium target, elucidating the mechanisms governing particle size and shape modulation across multiple pulses. Amir R. Sadrolhossini et al.[20] recently employed laser ablation techniques to synthesize titanium oxide nanoparticles in an aqueous solution containing carbon. Recently, Salman et al.[21] synthesized TiO_2 nanoparticles using pulsed laser ablation of a titanium target submerged in double-distilled deionized water, utilizing a 532 nm wavelength Nd:YAG laser with an energy output of 500 mJ. The synthesized TiO_2 nanoparticles exhibited a straight optical transition with a band gap of 3.65 eV.

In this research, titanium powder is pressed into a pellet, then bombarded with a laser underwater with different laser energy to produce titanium nanoparticles. After that, they are deposited on a glass substrate using spin coating for testing. Particle size distribution, crystallinity, and optical band-gap properties are all significantly influenced by laser energy (fluence). The present study assessed the impact of laser energy on the physical properties of synthesized TiO_2 thin film nanoparticles.

2. EXPERIMENTAL

2.1 Preparation of TiO_2 Thin Film Nanoparticles

The powder of Titanium Dioxide (TiO_2, ≥99.5% purity) is pressed into pellets with a diameter of 1 cm and a thickness of 0.4 cm using a hydraulic piston-type press (SPECAC) at 5 tons for 10 minutes. Titanium is immersed in deionised water (DDDW) (2 mL) in a glass beaker. Nd: YAG laser (Huafei Tongda Technology—DIAMOND-288 pattern EPLS) is used to prepare TiO2 thin film nanoparticle, providing pulses of 1064nm wavelength with different energy per pulse of (50, 100, 150, 250) mJ, pulse width of 10ns, repetition rate of 10Hz and effective beam diameter of 5mm, number of pulses of 800 pulse is used for laser ablation. The laser ablation process in deionised water is continuous for 5

minutes. During laser irradiation of the TiO_2 pellets, the plume of plasma is clearly visible to the naked eye. This is because of the ablation procedure. Spin coating is used to deposit thin films of TiO_2 nanoparticles prepared with different energy per pulse (50, 100, 150, 250 mJ) on a glass substrate. The structural type, grain size and morphology of the thin films are examined using UV-vis spectroscopy, X-ray diffraction and atomic force microscopy. A schematic diagram of Experimental Methods is shown in Figure 1.

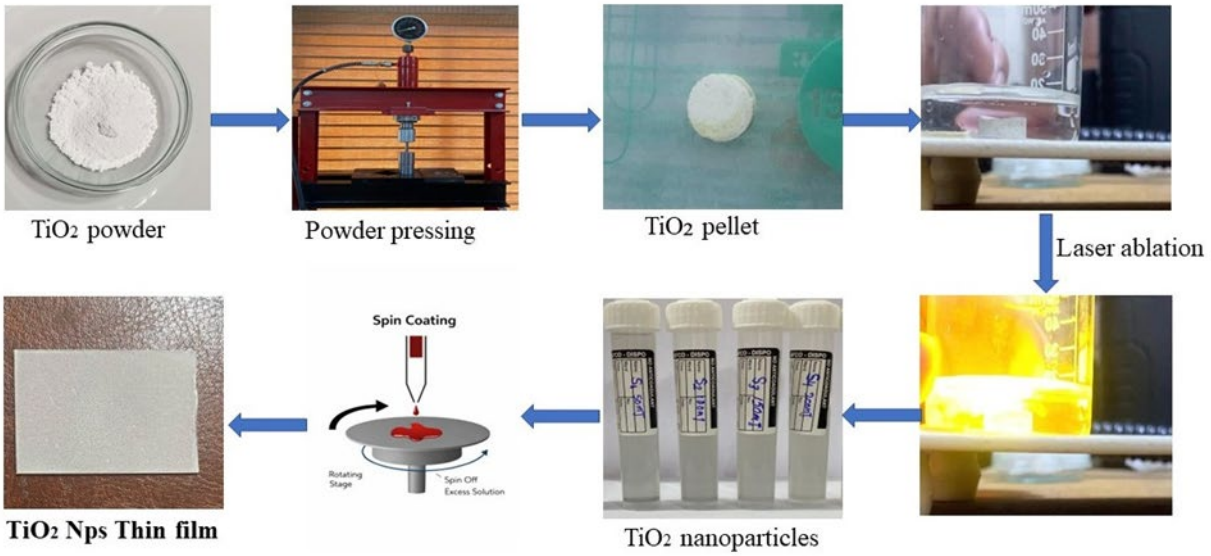

Figure 1 Schematic diagram of experimental method.

2.2 Characterization

The morphology and structure of the TiO_2 NPs thin films are evaluated by the Field Emission - Scanning Electron Microscopy (FE-SEM) and X-ray diffraction (XRD). In the present work, an X-ray diffractometer type (Miniflex II), with a Cu-Kα X-ray tube (λ = 1.54056 Å) is used. And using FESEM (model: ZEISS LIGMA Series). A UV/Visible spectrophotometer type SP-8001 is used to study the optical properties of TiO_2 thin films NPs in the wavelength range 300-1100 nm.

3. RESULTS AND DISCUSSION

3.1 XRD analysis

XRD patterns of TiO_2 thin films nanoparticles synthesized via laser ablation in deionized water at different laser energies are obtained, and the films are then deposited onto the glass substrate separately. Figure.2 shows the XRD pattern of the TiO_2 NPs Thin film prepared at laser energies of 50, 100, 150, and 250 mJ. All diffraction patterns exhibit characteristic peaks corresponding to the rutile phase (Tetragonal crystal structure) of TiO_2, in good agreement with the standard JCPDS card No. 96-900-4143. There are no peaks for anatase or brookite; this indicates that the laser ablation conditions promoted the transformation to rutile even in deionized water. The dominate peak at 2Θ = 27.4306º, 35.959º, 39.197º, 41.25º, 44.07º, 54.44º, 56.903º, 61.997º, 64.01º, 69.6º) which corresponds to the Braggs reflection plane of (110), (101), (200), (111), (210), (211), (220), (002), (310), (112). The crystallite Sizes (nm) are calculated using the Scherrer equation [22] based on the most intense peak (110) of the rutile phase, as shown in Table 1 below.

Table 1. Illustrates the structural parameters 2θ, FWHM, and crystallite size of TiO_2 thin film nanoparticles at different laser energies.

Laser energy	2Θ	FWHM	Crystallite Size (nm)
50 mJ	27.497º	0.83214	9.8
100 mJ	27.447º	0.48477	16.9
150 mJ	27.478º	0.46423	17.6
250 mJ	27.497º	0.28025	29.2

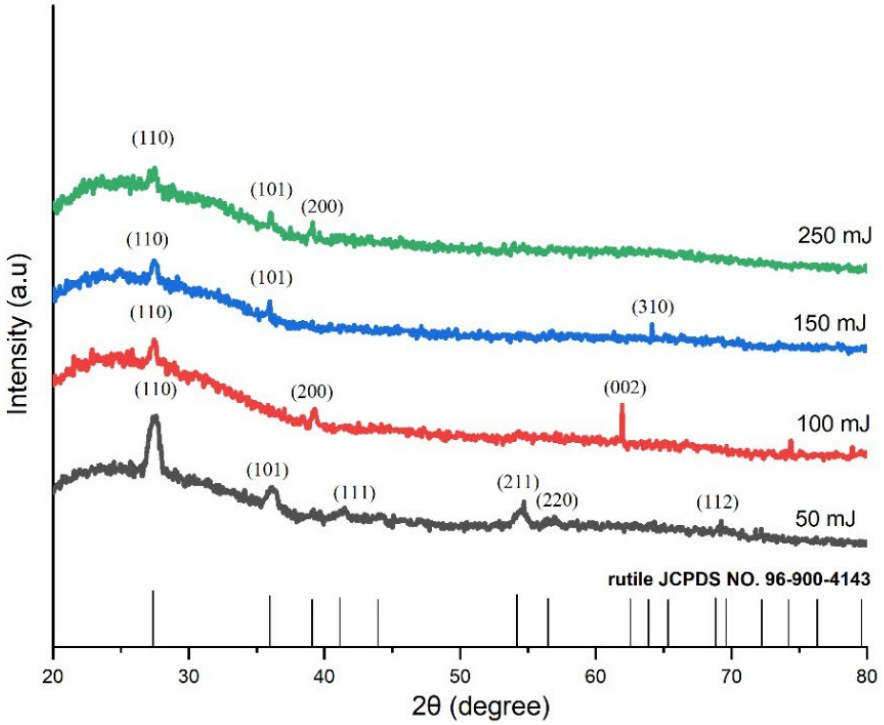

Figure 2 XRD spectra of the TiO_2thin films NPs prepared at different laser energies.

The full width at half maximum (FWHM) decreased and the diffraction peaks became sharper as the laser energy increased, indicating increased crystallinity and crystallite development. The plasma density and energy above the target surface increase with increasing laser energy, resulting in higher temperatures and instantaneous pressures within the plasma. These high-energy conditions provide the discharged atoms and ions with sufficient kinetic energy to facilitate atomic rearrangement during condensation in the liquid [20]. Consequently, crystal imperfections are diminished, enhancing the likelihood of orderly crystal nucleation and growth. Moreover, enhanced crystal ordering and larger crystallites are achieved through laser-induced remelting and subsequent recrystallisation of the resultant nanoparticles. The rutile phase exhibits greater stability at higher energies, resulting in shorter diffraction peaks and less lattice strain [23].

3.2 Field Emission- Scanning Electron Microscopy (FE-SEM)

Figure 3 presents the FE-SEM images of TiO_2 thin film nanoparticles synthesised via pulsed laser ablation at different laser energies a) 8 mJ, b) 120 mJ, and c) 160 mJ in deionised water. The images show that the synthesised nanoparticles display a uniform distribution and a spherical/quasi-spherical morphology, showcasing a novel shape that differs from the nanoparticle configurations generated by the PLAL technique in previous studies, where most particles are interconnected, resulting in nanoparticle clusters (Figure 3 a-c). All samples had a symmetrical morphology, with nanoparticle size increasing with increasing laser intensity. The morphological parameters derived from FE-SEM analysis of each examined region are displayed in Table 2.

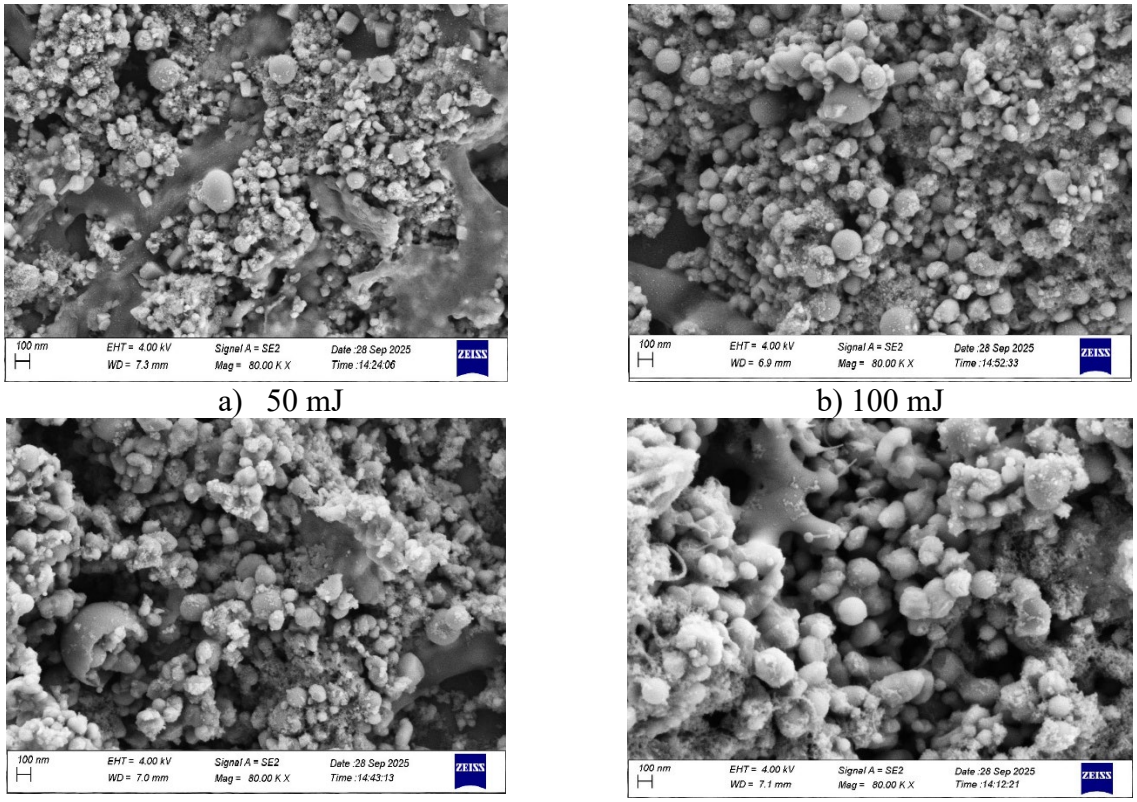

Figure 3 FE-SEM image of TiO_2thin films NPs synthesized via pulsed laser ablation at different laser energies.

Table 2. Illustrates the morphological parameters derived from FE-SEM analysis.

Laser energies	Average particle size (nm)	Morphological
50	20-25	Clear clustering, wide size distribution
100	25-50	Denser packing and stronger agglomeration
150	35-60	Uneven distribution, medium clustering
250	50-70	Particles are slightly more distinguishable with strong agglomeration

3.3 UV–Visible spectroscopy

The UV-vis spectrum of TiO_2 NPs synthesized via laser ablation in deionized water at different laser energies (50, 100, 150, and 250) eV is obtained. Figure 4a shows the UV-Vis optical absorption spectrum of the samples for different laser energies. It is an exhibit absorption band at 295, 298, 297, and 296 nm for 50, 100, 150, and 250 eV, respectively. From these bands of absorption, noticed that the absorption increased as the laser energy increased. To measure the optical band-gap of samples, Tauc's relationship is used as follows [24-26]:

$$(\alpha h\upsilon) = B\,(h\upsilon - Eg)^r \quad (1)$$

where α refers to the coefficient of absorption; h is the Planck constant; $h\upsilon$ is the incident photon energy; B is a constant and it known as the Tauc's parameter; Eg represents for the energy band-gap; and r refers to a coefficient which depends on the type of electronic transition; it can take two values 1/2 or 2 depending on the transition whether direct transition or indirect transition. By drawing $(\alpha h\upsilon)^2$ against $h\upsilon$, the linear line obtained refers to the energy band-gap of TiO_2 NPs samples after intersecting with the $h\upsilon$ axis. Figure 4b shows that the transitions are direct and the band-gaps are 3, 3.7, 3.5, and 3.65 eV, corresponding to the samples that are laser ablated by 50, 100, 150, and 250 eV, respectively.

The wide values of band-gap energies of TiO_2 NPs, consistent with the rutile structure, are due to confinement effects. When the particle size is very small, the band-gap is high. The optical properties and wide band-gap energies of TiO_2 NPs enable many applications, such as Photocatalysis, Materials Science, Sensors, Optics and Coatings [27-29].

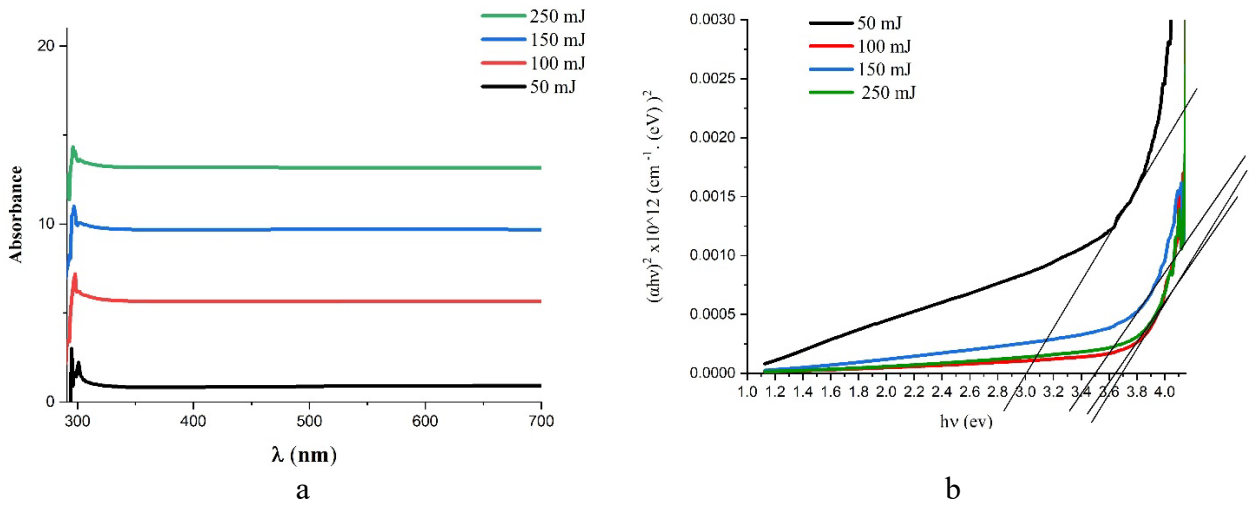

Figure 4 a) UV–visible absorption spectra, b) Optical band-gaps of TiO_2 NOs synthesized via laser ablation at different laser energies (50, 100, 150, and 250) mJ.

4. CONCLUSIONS

In summary, we successfully synthesised TiO_2 thin-film nanoparticles with unique crystal characteristics using pulsed laser ablation of an immersed TiO_2 pellet in deionised water (PLAL). This method makes the process easier, more flexible, more successful, and more cost-effective. The X-ray diffraction (XRD) patterns of TiO_2 thin film nanoparticles indicate the growth of the rutile phase. Increased laser energy improves the clarity of the diffraction peaks and reduces the full width at half maximum (FWHM), indicating enhanced crystallinity and larger crystallite size. The FESEM image

indicates that all samples include spherical to quasi-spherical nanoparticles, exhibiting noticeable agglomeration. The nanoparticles exhibit uniform shape, with the majority measuring 20-70 nm. At different laser energies, the samples' UV-Vis absorption spectra were obtained. Absorption bands indicated the absorption increased with increasing laser energy. The absorption band is observed at 295, 298, 297, and 296 nm for energy levels of 50, 100, 150, and 250 mJ, respectively.

References

[1] S.M. Gupta, M. Tripathi, Chinese Sci. Bull. 56 (2011) 1639 https://doi.org/10.1007/s11434-011-4476-1
[2] O.U. Akakuru, Z.M. Iqbal, A. Wu, Appl. Nanobiotechnology Nanomedicine (2020) 1 https://doi.org/10.1002/9783527825431.
[3] R. Sahnoun, Exp. Theor. Nanotechnol. 7 (2023) 78 https://doi.org/10.56053/7.2.78
[4] F. Pellegrino, L. Pellutiè, F. Sordello, C. Minero, E. Ortel, V.-D. Hodoroaba, V. Maurino, Appl. Catal. B Environ. 216 (2017) 80 https://doi.org/10.1016/j.apcatb.2017.05.046
[5] K.S. Shalini Devi, Xiong, S. Tsujimura, Appl. Heal. Energy Environ., Springer, 2025: pp. 339 https://doi.org/10.1007/978-3-031-80625-4
[6] F. Irfan, M.U. Tanveer, M.A. Moiz, S.W. Husain, M. Ramzan, Eur. Phys. J. B 95 (2022) 184 https://doi.org/10.1140/epjb/s10051-022-00440-8
[7] E.M. Samsudin, S.B. Abd Hamid, Appl. Surf. Sci. 391 (2017) 326 https://doi.org/10.1016/j.apsusc.2016.07.007
[8] N. Geetha, S. Sivaranjani, A. Ayeshamariam, M.K. Micheal, D. Saravankkumar, S.A. Fowziya, A.M. Mohideen, M. Jayachandran, J. Adv. Microsc. Res. 13 (2023) 3 https://doi.org/10.1515/gps-2023-0076
[9] S. Saravanan, R.S. Dubey, Mater. Today Proc. 47 (2021) 1811 https://doi.org/10.1016/j.matpr.2021.03.207
[10] A. Prathan, J. Sanglao, T. Wang, C. Bhoomanee, P. Ruankham, A. Gardchareon, D. Wongratanaphisan, Sci. Rep. 10 (2020) 8065 https://doi.org/10.1038/s41598-020-64510-6.
[11] M. Taylor, R.C. Pullar, I.P. Parkin, C. Piccirillo, J. Photochem. Photobiol. A Chem. 400 (2020) 112727 https://doi.org/10.1016/j.jphotochem.2020.112727
[12] S. Goulart-Gonçalves, M. de Souza-Pereira, R.M. Benetti, G.C. Bellettini, F. Elyseu, A.G. Dal-Bó, A.M. Bernardin, J. Phys. Chem. Solids 180 (2023) 111368 https://doi.org/10.1016/j.jpcs.2023.111368
[13] W. Gibbs, M. Torris, Exp. Theor. Nanotechnol 3 (2019) 103 https://doi.org/10.56053/3.1.103
[14] M.N. Morshed, X. Shen, H. Deb, S. Al Azad, X. Zhang, R. Li, J. Nat. Fibers 33 (2020) 57 https://doi.org/10.1080/15440478.2018.1465506
[15] K.S. Khashan, G.M. Sulaiman, F.A. Abdulameer, S. Albukhaty, M.A. Ibrahem, T. Al-Muhimeed, A.A. AlObaid, Appl. Sci. 11 (2021) 4623 https://doi.org/10.3390/app11104623.
[16] D. Blažeka, J. Car, N. Krstulović, Materials 15 (2022) 3146 https://doi.org/10.3390/ma15093146
[17] F. Barreca, N. Acacia, E. Barletta, D. Spadaro, G. Curro, F. Neri, Appl. Surf. Sci. 256 (2010) 6408 https://doi.org/10.1016/j.apsusc.2010.04.026
[18] A. Singh, J. Vihinen, E. Frankberg, L. Hyvärinen, M. Honkanen, E. Levänen, J. Ceram. Sci. Technol. 8 (2017) 39 https://doi.org/10.4416/JCST2016-00071.
[19] Z. Huang, G. Feng, K. Zhou, J. Han, Z. Shi, C. He, N. Xie, Q. Zhang, Opt. Express 30 (2022) 20482 https://doi.org/10.1364/OE.455658
[20] A.R. Sadrolhosseini, M. Beygisangchin, S. Shafie, S.A. Rashid, H. Nezakati, Mater. Res. Express 8 (2021) 105003 https://doi.org/10.1088/2053-1591/abdf0f.
[21] A.A. Salman, Eng. Technol. J. 34 (2016) 100 https://doi.org/10.30684/etj.34.1B.12
[22] R.M. Abdallah, R.M.S. Al-Haddad, J. Phys. Conf. Ser., IOP, 2021, 12022 https://doi.org/10.1088/1742-6596/1829/1/012022.

[23] Z. Wang, S.K. Saxena, V. Pischedda, H.P. Liermann, C.S. Zha, J. Phys. Condens. Matter 13 (2001) 8317 https://doi.org/10.1088/0953-8984/13/36/307
[24] K.M. Ibrahim, W.R. Saleh, A.Y. Taradh, J. Ovonic Res. 21 (2025) 761 https://doi.org/10.15251/JOR.2025.216.761
[25] A. I. A. Ali, M. RASHEED, Experimental and Theoretical NANOTECHNOLOGY 10 (2026) 277 https://doi.org/10.56053/10.s.277
[26] A. Khaleefah, M. RASHEED, Experimental and Theoretical NANOTECHNOLOGY 10 (2026) 289 https://doi.org/10.56053/10.s.289
[27] Z. S. Ahmed, M. RASHEED, H. S. Ahmed, Experimental and Theoretical NANOTECHNOLOGY 10 (2026) 329 https://doi.org/10.56053/10.s.329
[28] Z. S. Ahmed, M. RASHEED, H. S. Ahmed, Experimental and Theoretical NANOTECHNOLOGY 10 (2026) 343 https://doi.org/10.56053/10.s.343.
[29] A. I. A. Ali, M. RASHEED, Experimental and Theoretical NANOTECHNOLOGY 10 (2026) 239 https://doi.org/10.56053/10.s.239.